Asian Journal of Chemistry; Vol. 37, No. 11 (2025), 2876-2882
ASIAN JOURNAL OF CHEMISTRY
https://doi.org/10.14233/ajchem.2025.34742

# Novel Indole Clubbed Thiazolidinediones as Inhibitors of Protein Tyrosine Phosphatase 1B (PTP1B)

JISHA PREMS[1,2,*], A. ANTON SMITH[1] and M.L. LAL PRASANTH[2]

[1]Department of Pharmacy, Annamalai University, Annamalai Nagar-608002, India
[2]Dr. Moopen's College of Pharmacy, Naseera Nagar, Wayanad-673577, India

*Corresponding author: E-mail: jishaprems28@gmail.com

*Received*: 22 August 2025 *Accepted*: 13 October 2025 *Published online*: 27 October 2025 AJC-22178

The escalating challenge in the carbohydrate metabolic disorders like diabetes mellitus in the modern era necessitates the development of antidiabetic agents that work on the unexplored pathways. In this study, the synthesis of a novel series of indole clubbed thiazolidinediones (**TN01-TN08**) for protein tyrosine phosphatase 1B (PTP1B) inhibition as insulin sensitizers for antidiabetic therapy is presented. The molecular hybridization approach was utilized to synthesize the analogues and FT-IR, $^{1}$H NMR, $^{13}$C NMR and LC-MS were employed to determine the structures of the newly synthesized compounds. The interaction mechanisms with the receptor, binding free energy and amino acid residues of the receptor enzyme involved in the interactions with different analogs were evaluated using molecular docking. The cytotoxic effects of synthesized compounds were assessed by MTT assay on HepG2 cell lines. Based on the cytotoxic assay, compounds were further treated with rat L6 myotubes as a model system to investigate peripheral insulin resistance and uptake of glucose by the cells. Further, selected compounds were subjected to an *in vitro* PTP1B inhibitory assay and most potential PTP1B inhibition was demonstrated by analogues **TN05** and **TN04** ($IC_{50}$ 28.52 and 32.67 respectively), which could further develop as therapeutically significant antidiabetic candidates.

**Keywords: PTP1B inhibition, Indole, Thiazolidinedione, Antidiabetic activity, Molecular docking.**

## INTRODUCTION

Diabetes mellitus is characterized by persistent hyperglycemia, defective insulin release from stored vacuoles, impaired insulin response or a combination of these factors, leading to dysregulation of glucose homeostasis in both heaptic and peripheral tissues over an extended duration [1]. Common clinical indicators of diabetes often include increased urination, fatigue, dehydration, increased hunger and excessive thirst. However, when type 2 diabetes mellitus (T2DM) is not adequately managed, it can lead to a range of severe complications that affect numerous body systems. Insulin resistance is a common characteristic of diabetes mellitus type 2 and obesity, two conditions that are increasingly prevalent across the globe [2]. Protein tyrosine phosphatase 1B (PTP1B), belonging to the class of protein tyrosine phosphatases (PTP), which is ubiquitously expressed in humans, is a negative regulator of insulin signaling, contributing significantly to the onset of diabetes and obesity [3].

Indole-based heterocycles represent a promising avenue in the development of novel antidiabetic agents due to the electron-rich nature of the indole ring significantly contributes to its ability to bind effectively with target proteins like PTP1B [4]. This characteristic property of indole facilitates favourable interactions like conventional H-bonding, π-π stacking, π-alkyl and other non-covalent interactions, with electron-deficient regions or aromatic amino acid residues within the active pocket of the enzyme, thereby increasing binding affinity with receptor [4]. Thiazolidinediones (TZDs), generally termed as glitazones, represent a significant class of oral antihyperglycemic agents employed as a choice of therapy for type 2 diabetes mellitus. The primary mode of action of glitazones involves enhancing insulin sensitivity in key peripheral tissues, including the liver, adipose tissue, and skeletal muscle [5]. Considering the diverse pharmacological activities associated with indole and thiazolidinedione (TZD) moieties and employing the molecular hybridization strategy, a series of novel indole clubbed thiazolidinediones was delib-

erately designed by integrating these crucial chemical features believed to be vital for effectively inhibiting the PTP1B enzyme. Consequently, the present investigation details the synthesis, *in silico* screening and *in vitro* biological evaluation of these novel indole clubbed thiazolidinediones as potential inhibitors of the PTP1B enzyme.

## EXPERIMENTAL

The chemicals and reagents used for the synthesis were obtained from Sigma-Aldrich, USA. The progress of the reactions was monitored by TLC using pre-coated silica 60 $F_{254}$ on aluminium sheets with a developing solvent system of *n*-hexane:ethyl acetate in varying ratios and spots were viewed under UV light. Melting points were determined by filling samples in one end sealed capillaries with Labtronics LT-115 electrically heated melting point apparatus. Infrared spectra (IR) were recorded on a Perkin-Elmer FTIR model PC spectrophotometer with frequency of absorptions reported in wave numbers. Employing deuterated dimethyl sulfoxide (DMSO-$d_6$) as solvent and tetramethyl silane (TMS) as internal standard, $^1$H and $^{13}$C NMR spectra were obtained at ambient temperature (298 K) on a Bruker AV-400 MHz spectrometer equipped with a multinuclear inverse probe head with gradient. In comparison with TMS (0.00 ppm), the chemical shifts were expressed in parts per million (ppm). Utilizing a Waters LC-MS/MS (USA), the mass spectra were recorded.

**Synthesis of 5-(substituted benzylidene)thiazolidine-2,4-diones:** A solution of thiazolidine-2,4-dione (8.1 mmol), substituted benzaldehyde (8.2 mmol) and benzoic acid (2.0 mmol) in toluene (8.0 mL) was heated to 40 ºC until it completely dissolved in a reaction flask equipped with a magnetic stirrer. This clear solution was immediately mixed with piperidine (2.0 mmol) and the reaction mixture was refluxed for 6 h. After filtering, washing, drying and recrystallization from ethanol, purified crystalline solids of 5-(substituted benzylidene)thiazolidine-2,4-diones were obtained [6].

**Synthesis of indole-thiazolidine-2,4-dione hybrid analogues (TN01-TN08):** 5-(Substituted benzylidene)thiazolidine-2,4-diones were condensed with 2-chloromethyl indole in the presence of NaOH in anhydrous DMF to generate the indole-thiazolidine-2,4-dione hybrid analogues (**TN01-TN08**). In a reaction flask, a mixture of 5-(substituted benzylidene)-thiazolidinedione (1.5 equiv.) and NaH (2.0 equiv.) was stirred vigorously at nitrogen atmosphere for 30 min at room temperature. Overnight stirring was maintained after adding 2-chloromethyl indole (1.5 equiv.) to this mixture. Using a mobile phase of *n*-hexane:ethyl acetate (1:1), TLC was used to track the progress of chemical synthesis. After completing the entire reaction time, the reaction mixture was added to crushed ice and the resultant precipitate was filtered and dried. (**Scheme-I**). Finally, the products were recrystallized from an appropriate ratio of chloroform:methanol solvent mixture to obtain the synthesized compounds in the purest form [7].

**(*E*)-3-((1*H*-indol-2-yl)methyl)-5-(4-dimethylaminobenzylidene)thiazolidine-2,4-dione (TN01):** m.f.: $C_{21}H_{19}N_3O_2S$; off-white solid; yield: 61%; m.p.: 264-265 ºC. FTIR (KBr, $\nu_{max}$, cm$^{-1}$): 3442.76 (N-H), 3048.37 (=C-H), 2982.39 (C-H), 1843.49 (C=O), 1824.83 (C=O), 1583.83 (N-O), 1265.72 (C-N); $^1$H NMR (400 MHz, DMSO-$d_6$) δ ppm: 11.67 (s, 1H, N*H*), 8.04 (s, 1H, Ar*H*), 7.51 (m, 1H, Ar*H*), 7.46 (m, 2H, Ar*H*), 7.28 (m, 1H, Ar*H*), 7.10 (m, 1H, Ar*H*), 7.06 (m, 1H, Ar*H*), 6.83 (m, 2H, Ar*H*), 6.22 (s, 1H, Ar*H*), 5.38 (s, 2H, C$H_2$), 3.08 (s, 6H, N(C$H_3$)$_2$); $^{13}$C NMR (DMSO-$d_6$) δ ppm: 163.52, 153.75, 145.33, 140.43, 139.43, 137.43, 125.12, 123.32, 123.11, 124.23, 120.53, 117.52, 115.62, 112.48, 107.43, 106.98, 65.46, 41.25.

**(*E*)-3-((1*H*-Indol-2-yl)methyl)-5-(4-aminobenzylidene)-thiazolidine-2,4-dione (TN02):** m.f.: $C_{19}H_{15}N_3O_2S$; white solid; yield: 76%; m.p.: 237-238 ºC. FTIR (KBr, $\nu_{max}$, cm$^{-1}$): 3561.45 (N-H), 3485.32 (N-H), 3069.48 (=C-H), 2943.76 (C-H), 1795.34 (C=O), 1831.93 (C=O), 1554.36 (N-O), 1200.43 (C-N); $^1$H NMR (400 MHz, DMSO-$d_6$) δ ppm: 11.21 (s, 1H, N-*H*), 8.21 (s, 1H, Ar*H*), 7.83 (m, 1H, Ar*H*), 7.64 (m, 2H, Ar*H*), 7.62 (m, 1H, Ar*H*), 7.32 (m, 1H, Ar*H*), 7.14 (m, 1H, Ar*H*), 6.73 (m, 2H, Ar*H*), 6.43 (s, 1H, Ar*H*), 5.42 (s, 2H, N$H_2$) 5.13 (s, 2H, C$H_2$); $^{13}$C NMR (DMSO-$d_6$) δ ppm: 165.64, 162.83, 148.54, 142.60, 138.78, 132.73, 128.94, 127.69, 126.84, 126.09, 124.53, 120.64, 119.45, 117.52, 112.48,108.34, 108.23, 59.34.

**(*E*)-3-((1*H*-Indol-2-yl)methyl)-5-(4-hydroxybenzylidene)thiazolidine-2,4-dione (TN03):** m.f.: $C_{19}H_{14}N_2O_3S$; cream solid; yield: 81%; m.p.: 263-265 ºC. FTIR (KBr, $\nu_{max}$, cm$^{-1}$): 3572.11 (O-H), 3434.84, (N-H), 3012.72 (=C-H), 2949.23 (C-H), 1772.71 (C=O), 1748.15 (C=O), 1576.22 (N-O), 1273.93 (C-N). $^1$H NMR (400 MHz, DMSO-$d_6$) δ ppm: 11.82 (s, 1H, N*H*), 10.47 (s, 1H, O*H*) 8.17 (s, 1H, Ar*H*), 7.74 (m, 1H, Ar*H*), 7.58 (m, 2H, Ar*H*), 7.53 (m, 1H, Ar*H*), 7.47 (m, 1H, Ar*H*), 7.23 (m, 1H, Ar*H*), 6.92 (m, 2H, Ar*H*), 6.83 (s, 1H, Ar*H*), 5.13 (s, 2H, C$H_2$). $^{13}$C NMR (DMSO-$d_6$) δ ppm: 173.23, 164.43, 152.74, 144.76, 140.23, 139.45, 131.83, 129.64, 128.72, 128.03, 125.23, 121.32, 119.82, 114.32, 113.45, 110.65, 103.87, 62.23.

**(*E*)-3-((1*H*-Indol-2-yl)methyl)-5-(4-methylbenzylidene)-thiazolidine-2,4-dione (TN04):** m.f.: $C_{20}H_{16}N_2O_2S$; white solid;

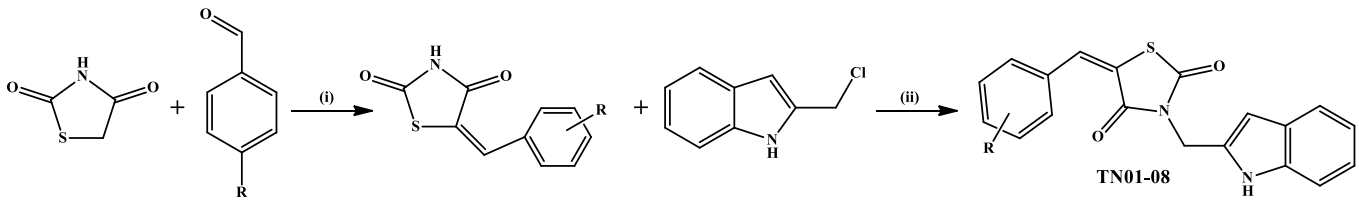


**Scheme-I:** Synthetic methods and reaction conditions used to prepare 1-(*H*)-indol-2-yl)methyl substituted 5-benzylidene-2,4-thiazolidinediones (**TN01-08**)

yield: 69%; m.p.: 287-288 ºC. FTIR (KBr, $\nu_{max}$, $cm^{-1}$): 3519.65 (N-H), 3054.93 (=C-H), 2923.92 (C-H), 1764.14 (C=O), 1743.23 (C=O), 1543.23 (N-O), 1265.82 (C-N); $^1$H NMR (400 MHz, DMSO-$d_6$) δ ppm: 11.19 (s, 1H, N*H*), 8.08 (s, 1H, Ar*H*), 7.65 (d, 2H, Ar*H*), 7.47 (d, 1H, Ar*H*), 7.40 (d, 2H, Ar*H*), 7.33 (d, 2H, Ar*H*), 7.18 (d, 1H, Ar*H*), 7.10 (t, 1H, Ar*H*), 7.06 (t, 1H, Ar*H*), 6.65 (s, 1H, Ar*H*), 5.06 (s, 2H, C$H_2$), 2.41 (s, 3H, C$H_3$); $^{13}$C NMR (DMSO-$d_6$) δ ppm: 173.39, 164.54, 142.38, 139.93, 137.76, 134.34, 129.59, 129.49, 128.93, 121.64, 120.62, 119.92, 114.73, 113.83, 103.82, 50.73, 22.47.

**(*E*)-3-((1*H*-Indol-2-yl)methyl)-5-(4-nitrobenzylidene)-thiazolidine-2,4-dione (TN05):** m.f.: $C_{19}H_{13}N_3O_4S$; intense yellow solid; yield: 74%; m.p.: 269-270 ºC. FTIR (KBr, $\nu_{max}$, $cm^{-1}$): 3602.11 (N-H), 3092.63 (=C-H), 2963.38 (C-H), 1753.26 (C=O), 1662.27 (C=O), 1573.19 (N-O), 1344.23 (N-O), 1238.17 (C-N); $^1$H NMR (400 MHz, DMSO-$d_6$) δ ppm: 11.60 (s, 1H, N*H*), 8.35 (d, 2H, Ar*H*), 8.14 (s, 1H, =C*H*), 8.05 (d, 2H, Ar*H*), 7.53 (d, 1H, Ar*H*), 7.36 (t, 1H, Ar*H*), 7.13 (t, 1H, Ar*H*), 7.06 (t, 1H, Ar*H*), 7.10 (t, 1H, Ar*H*), 7.06 (t, 1H, Ar*H*), 6.22 (s, 1H, Ar*H*), 5.02 (s, 2H, C$H_2$); $^{13}$C NMR (DMSO-$d_6$) δ ppm: 172.20, 163.94, 146.18, 141.63, 139.46, 135.43, 133.73, 129.53, 129.27, 128.56, 123.65, 121.54, 120.73, 119.46, 116.56, 111.13, 101.59, 49.98.

**(*E*)-3-((1*H*-Indol-2-yl)methyl)-5-(4-bromobenzylidene)-thiazolidine-2,4-dione (TN06):** m.f.: $C_{19}H_{13}BrN_2O_2S$; pale pink solid; yield: 74%; m.p.: 297-299 ºC. FTIR (KBr, $\nu_{max}$, $cm^{-1}$): 3484.56 (N-H), 3056.49 (=C-H), 2914.58 (C-H), 1739.26 (C=O), 1722.62 (C=O), 1252.78 (C-N), 1072 (C-Br); $^1$H NMR (400 MHz, DMSO-$d_6$) δ ppm: 11.29 (s, 1H, N*H*), 8.16 (s, 1H, =C*H*), 7.73 (d, 2H, Ar*H*), 7.63 (d, 2H, Ar*H*), 7.45 (d, 1H, Ar*H*), 7.26 (t, 1H, Ar*H*), 7.12 (t, 1H, Ar*H*), 7.08 (t, 1H, Ar*H*), 7.01 (t, 1H, Ar*H*), 6.56 (s, 1H, Ar*H*), 4.86 (s, 2H, C$H_2$). $^{13}$C NMR (DMSO-$d_6$) δ ppm: 173.23, 165.38, 143.4, 136.49, 136.46, 134.27, 131.48, 128.25, 128.20, 123.43, 122.26, 121.38, 120.38, 118.27, 114.30, 109.75, 102.58, 48.44.

**(*E*)-3-((1*H*-Indol-2-yl)methyl)-5-(4-chlorobenzylidene)-thiazolidine-2,4-dione (TN07):** m.f.: $C_{19}H_{13}ClN_2O_2S$; white solid; yield: 72%; m.p.: 245-247 ºC. FTIR (KBr, $\nu_{max}$, $cm^{-1}$): 3415.49 (N-H), 1732.33 (C=O), 1683.83 (C=O), 1603.59 (C=C), 1257.84 (C-N), 1150.07 (C-S), 1089.54 (C-Cl), $^1$H NMR (400 MHz, DMSO-$d_6$) δ ppm: 11.09 (s, 1H, N*H*), 8.17 (s, 1H, =C*H*), 7.65 (d, 2H, Ar*H*), 7.60 (d, 2H, Ar*H*), 7.58 (d, 1H, Ar*H*), 7.37 (t, 1H, Ar*H*), 7.21 (t, 1H, Ar*H*), 7.14 (t, 1H, Ar*H*), 7.08 (t, 1H, Ar*H*), 6.38 (s, 1H, Ar*H*), 5.17 (s, 2H, C$H_2$). $^{13}$C NMR (DMSO-$d_6$) δ ppm: 175.87, 164.30, 147.69, 142.51, 138.82, 137.48, 133.47, 127.73, 126.86, 123.57, 121.98, 121.58, 120.49, 116.64, 113.72, 111.69, 101.63, 53.73.

**(*E*)-3-((1*H*-Indol-2-yl)methyl)-5-(4-fluorobenzylidene)-thiazolidine-2,4-dione (TN08):** m.f.: $C_{19}H_{13}FN_2O_2S$; pale yellow solid; yield: 68%; m.p.: 271-272 ºC. FTIR (KBr, $\nu_{max}$, $cm^{-1}$): 3459.59 (N-H), 1753.83 (C=O), 1717.48 (C=O), 1606.93 (C=C), 1268.49 (C-N), 1147.84 (C-S), 1224.59 (C-F), $^1$H NMR (400 MHz, DMSO-$d_6$) δ ppm: 11.28 (s, 1H, N*H*), 8.31 (s, 1H, =C*H*), 7.78 (d, 2H, Ar*H*), 7.66 (d, 2H, Ar*H*), 7.49 (d, 1H, Ar*H*), 7.32 (t, 1H, Ar*H*), 7.19 (t, 1H, Ar*H*), 7.12 (t, 1H, Ar*H*), 7.04 (t, 1H, Ar*H*), 6.40 (s, 1H, Ar*H*), 5.12 (s, 2H, C$H_2$). $^{13}$C NMR (DMSO-$d_6$) δ ppm: 170.69, 168.63, 145.73, 142.49, 137.52, 137.04, 131.94, 129.66, 129.07, 124.84, 121.59, 120.63, 118.58, 116.73, 114.73, 108.69, 102.72, 50.68.

**Cell viability assay:** Culture media from HepG2 cells exposed to various substances (**TN01-TN08**) were examined using 3-(4,5-dimethylthiazol-2-yl)-2,5-diphenyl-2*H*-tetrazolium bromide (MTT) assay to evaluate cell survival. Each test and control well received 30 μL of reconstituted MTT solution (5 mg/mL in phosphate-buffered saline, pH 7.4) after the 24 h incubation period. Then, the plate was gently oscillated on an orbital shaker and incubated in a humidified 5% $CO_2$ incubator at 37 ºC for 4 h. The MTT formazan, which was generated by metabolically viable cells, was dissolved in 150 μL of DMSO by mixing it for 30 min on an orbital shaker after the supernatant was aspirated. A 96-well microplate reader was used to directly obtain the absorbance values at 540 nm wavelength [8].

**Glucose oxidase-peroxide (GOD-POD) enzyme assay:** Using monolayers of L6 rat muscle cell lines, the colorimetric test method of glucose absorption was used to assess the impact of the synthesized hybrid compounds **TN01**-**TN08** on glucose uptake. L6 cell lines were grown into a sub-confluent monolayer in a 5% $CO_2$ incubator under humidified conditions at 37 ºC in a solution comprising of 10% fetal bovine serum, glucose (4.5 g/L), streptomycin (100 μg/L) and penicillin (100 U/mL) in Dulbecco's modified eagle medium (DMEM). Following the monolayer formation, the culture was reconstituted using serum-free DMEM with 0.2% bovine serum albumin (BSA) and incubated for 18 h at 37 ºC in a $CO_2$ incubator. After discarding the medium, cells were once again washed with Krebs-Ringer Phosphate (KRP) buffer. Test compounds (100 μg/mL), pioglitazone and insulin were then treated with the cells. After that a 1 M glucose solution was added and further incubated for 30 min. Then, the treated cells were washed three times using 1 mL of ice-cold KRP buffer to stop uptake of glucose and the supernatant was utilized for initial glucose estimation. All cells were lysed by subsequent freezing and thawing three times and the obtained cell lysate was used for estimating final glucose concentration. The change in the final glucose concentration from initial value was estimated based on GOD-POD enzyme assay kit, by incubating 10 μL of cell lysate or supernatant with 1 mL of GOD-POD assay reagent 10 min at 37 ºC [9,10].

**PTP1B enzyme inhibition assay:** The synthesized analogues underwent *in vitro* assessment for their ability to inhibit PTP1B using the PTP1B drug discovery kit BML-AK822 (Enzo Life Sciences, USA). The test relies on the scientific fact that PTP1B dephosphorylates the IR5 phosphopeptide substrate, which is formed from an amino acid sequence originating from the β subunit domain of the insulin receptor, necessitating autophosphorylation for the receptor kinase to become fully active [11]. This assay kit incorporates human recombinant PTP1B (amino acid residues 1-322; molecular weight 37,400 Da), produced in *E. coli*. Beyond the recombinant PTP1B, the kit provides the substrate (comprising IR5 insulin receptor residues of amino acids 1142-1153, pY1146, molecular weight 17,030 Da), phosphate quantifying reagent Biomol red, the assay buffer and a reference standard Suramin. The experimental procedures were executed, adhering to the manufacturer's protocol under appropriate laboratory conditions. Stock solutions of test compounds **TN01**, **TN04**, **TN05**, **TN07**, **TN08** and standard pioglitazone were prepared in

DMSO at five different concentrations (6.25, 12.5, 25, 50 and 100 µg/mL) [12].

An aliquot was prepared composed of 35 µL assay buffer warmed to 30 ºC, 10 µL of DMSO as control or 10 µL inhibitor/standard dissolved in DMSO at above mentioned concentrations and 5 µL diluted PTP1B enzyme in order to assess the PTP1B inhibitory activity of the synthesized compounds. Next, 50 µL of PTP1B substrate was added to start the reaction and the mixture was incubated for 0.5 h at 30 ºC. The addition of 25 µL of Biomol red reagent after the incubation time allowed the process to stop. After being shaken on an orbital shaker, the mixture was left to stand for roughly 0.5 h in order to develop colour. The absorbance was measured at 620 nm using Erba automated microplate ELISA reader (Erba Lisa Scan EM). The percentage inhibition of PTP1B enzyme activity by the test compounds was calculated relative to the control wells, which were considered to represent 100% activity. Assays were conducted in triplicate and for each sample, $IC_{50}$ values were calculated based on the linear regression method, as the assay gives a linear dose-response curve [13-15].

***In silico* molecular docking:** The RCSB Protein Data Bank (www.rcsb.org) provided the X-ray crystal structure of protein tyrosine phosphatase 1B at a resolution of 1.80 Å (PDB ID:1C83), existing as complexed with the natural inhibitor 6-(oxalyl-amino)-1*H*-indole-5-carboxylic acid. PyMOL software was used to prepare the downloaded 3D structure of protein for missing hydrogens, side-chain abnormalities and incorrect bonds. All of the ions, complex compounds, water molecules and natural inhibitor complexed to the proteins were eliminated. After uploading the optimized PDB structures to the AutoDock-MGL Tool, polar hydrogens were added and the PDBQT files were generated using the usual protocols [16].

The 3D structures of the ligands were optimized and Open Babel was used to convert the structures of ligands from .mol to PDB format. To obtain the PDBQT files, ligands were uploaded into AutoDock-MGL Tool and conventional procedures were followed; further, the Gasteiger charges were applied. A grid box with a grid spacing of 0.375 Å and a grid map of 60 × 60 × 60 points was made for each docking. The output file generated from the docking analysis includes the top seven binding poses along with their corresponding binding affinities in Kcal/mol. The ligand binding poses with the lowest root mean square deviation (RMSD) and the maximum binding affinity was chosen. Discovery Studio visualizer was used to visualize the protein-ligand interactions in both two and three dimensions. The 2D binding pattern displays the types of interactions between amino acid residues and the ligand and the 3D binding pattern indicates the precise location of the binding pocket on the target protein [17].

## RESULTS AND DISCUSSION

**Scheme-I** outlines the synthesis of the novel indole clubbed thiazolidinedione compounds. Substituted benzaldehydes were reacted with thiazolidine-2,4-dione *via* Knoevenagel condensation to synthesize 5-benzylidene substituted thiazolidine-2,4-diones. N-substitution of thiazolidinediones with an indole moiety was carried out by treating thiazolidinediones with sodium hydride, followed by the addition of 2-chloromethyl indole. The reaction mixture was placed into ice-cold water after the specified time period led to the formation of 1-(*H*)-indol-2-yl)methyl substituted 5-benzylidene-2,4-thiazolidinediones (**TN01-TN08**). The purity of compounds was verified by TLC (*n*-hexane/ethyl acetate mobile phases) and further purified using short column chromatography, yielding all target compounds **TN01-TN08** in pure form.

After purification, **TN01-TN08** were characterized with $^1$H NMR, $^{13}$C NMR and LC-MS. $^1$H NMR spectra of the synthesized hybrid compounds showed a methine proton signal between 8.08 to 7.94 ppm corresponding to an E-configuration [18]. The disappearance of the methylene proton signal around 4.65 further confirmed Knoevenagel condensation on thiazolidine-2,4-dione to obtain 5-benzylidene substituted thiazolidine-2,4-dione. The $-CH_2$ proton attached to the thiazolidine-2,4-dione resonated in the range of 5.03 to 5.11ppm confirmed the $SN^2$ reaction with 2-chloromethyl indole. These two signals are outstanding for the product structure confirmation.

**Cell viability assay:** In this study, the MTT assay was employed to assess the cytotoxic impact of novel synthesized benzimidazole-thiazolidinedione conjugates (**TN01-TN08**). Following a 24 h exposure of HepG2 cells to the evaluated compounds, no alterations in cell viability were observed, indicating that the concentrations utilized for this investigation did not compromise cellular integrity during the incubation period. Furthermore, treatment with the compounds did not influence cell proliferation, suggesting the maintenance of a normal cell cycle and the lack of any impact on the proliferative mechanisms. The findings from the cytotoxicity assessment performed on HepG2 cells are illustrated in Fig. 1.

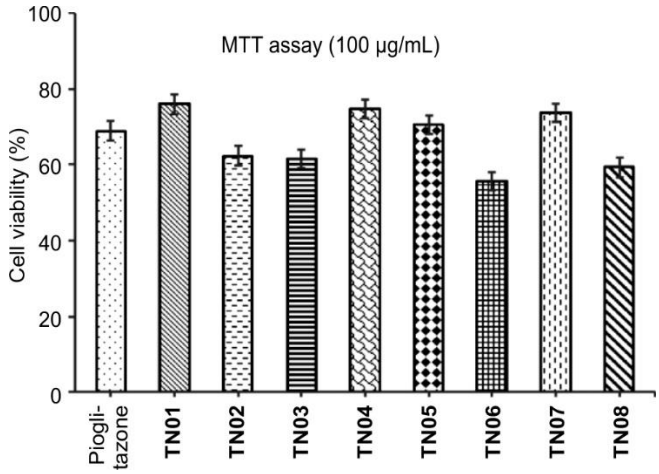


Fig. 1. Cell viability (%) of HepG2 cells assessed by MTT assay: Bar graphs depict the response to various test compounds (**TN01-08**) and pioglitazone at concentrations of 100 µg/mL. Three replicates of tests were run to calculate the mean value and represented as mean ± SD (n = 3)

**Glucose oxidase-peroxide (GOD-POD) enzyme assay:** The pivotal role of skeletal muscle in maintaining systemic glucose balance is affirmed by its capacity for insulin-stimulated glucose uptake, a process largely governed by the translocation of GLUT4 transporters to the cell membrane. Given this physiological significance, the current study employed differentiated L6 myotubes, a well-established *in vitro*

model, to meticulously investigate the effects of novel compounds on glucose uptake mechanisms and their potential to modulate insulin resistance [19]. The quantitative findings from the *in vitro* glucose uptake assays, visually represented in Fig. 2, distinctly indicate that compounds **TN04** and **TN05** elicited levels of glucose uptake activity that were comparable to that of the established reference compound. In contrast, the other synthesized molecules under investigation displayed a level of activity ranging from low to moderate in their ability to facilitate glucose uptake in this cellular model.

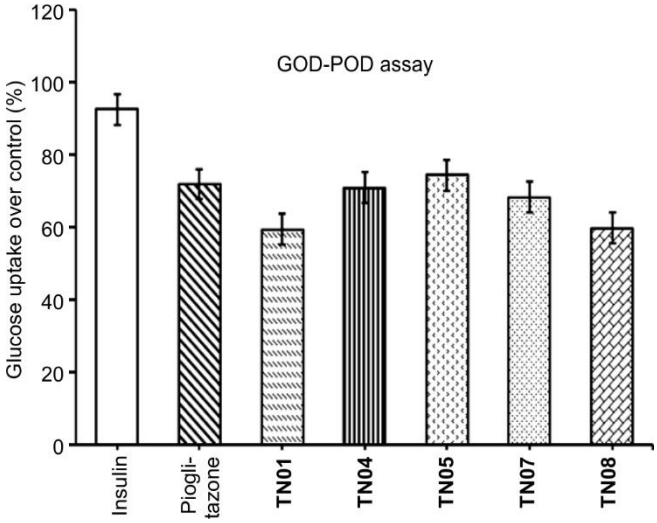


Fig. 2. Glucose uptake modulation by synthesized compounds (**TN01**, **TN04**, **TN05**, **TN07** and **TN08**) and pioglitazone in Insulin-treated L6 Myotubes. Three replicates of tests were run to calculate the mean value and represented as mean ± SD (n = 3)

**PTP1B enzyme inhibition assay:** To determine the structural features necessary for PTP1B inhibition, compounds were tested in a laboratory setting. This was done using the PTP1B colorimetric assay kit BML-AK822, with a reference standard suramin. This assay measured the effect of each compound on the release of inorganic phosphate from an IR5 phosphopeptide substrate.

***In silico* molecular docking:** The novel synthesized compounds bind at the active site of the target receptor PTP1B (PDB ID: 1C83) and the binding affinity of analogues was expressed as docking scores ranging from –8.1 to –6.4 kcal $mol^{-1}$ [20]. Among them, **TN05** exhibited the highest binding score of –8.1 kcal $mol^{-1}$, followed by **TN04** (–7.9 kcal $mol^{-1}$), **TN01** (–7.7 kcal $mol^{-1}$) and **TN07** (–7.6 kcal $mol^{-1}$) as shown in Table-1.

The *p*-dimethyl amino derivative (**TN01**) showed the remarkable interactions with the receptor active site through a conventional hydrogen bonding between indole N-H and Gln262, pi-pi stacking with Phe182, pi-alkyl interaction with Val49 and van der Waals interactions with residues Tyr46, Asp48 and Asp181. The *p*-methyl derivative (**TN04**) showed effective interactions with the receptor active site primarily through a conventional hydrogen bonding between indole N-H and Gln262, pi-pi stacking with Phe182, pi-sigma interaction with Ala 217, pi-alkyl interaction with Val49, Phe182 and Ala217. Furthermore, van der Waals interactions were observed with residues Tyr46 and Asp48 (Fig. 3a).

TABLE-1
*In vitro* PTP1B ENZYME INHIBITION (Mean ± SD, n = 3) AND *in silico* MOLECULAR DOCKING RESULTS OF DESIGNED COMPOUNDS ON COMPARISON TO THE STANDARD INSULIN SENSITIZER PIOGLITAZONE

| Compd. | Conc. (µM) | PTP1B inhibition (%) | $IC_{50}$ (µM) | Binding affinity (Kcal/mol) |
|---|---|---|---|---|
| **TN01** | 6.25 | 27.64 ± 0.51 | 57.40 | -7.7 |
| | 12.5 | 32.09 ± 0.24 | | |
| | 25 | 36.33 ± 0.72 | | |
| | 50 | 43.48 ± 0.65 | | |
| | 100 | 70.36 ± 0.78 | | |
| **TN04** | 6.25 | 31.35 ± 1.02 | 32.67 | -7.9 |
| | 12.5 | 45.63 ± 0.39 | | |
| | 25 | 51.45 ± 0.68 | | |
| | 50 | 60.62 ± 0.42 | | |
| | 100 | 74.25 ± 0.27 | | |
| **TN05** | 6.25 | 35.45 ± 0.97 | 28.52 | -8.1 |
| | 12.5 | 40.07 ± 0.37 | | |
| | 25 | 52.21 ± 0.69 | | |
| | 50 | 68.20 ± 1.61 | | |
| | 100 | 76.15 ± 0.44 | | |
| **TN07** | 6.25 | 32.45 ± 0.61 | 36.89 | -7.6 |
| | 12.5 | 39.07 ± 0.35 | | |
| | 25 | 47.21 ± 0.81 | | |
| | 50 | 60.20 ± 0.45 | | |
| | 100 | 75.15 ± 0.47 | | |
| **TN08** | 6.25 | 28.94 ± 0.92 | 59.04 | -6.4 |
| | 12.5 | 33.53 ± 0.33 | | |
| | 25 | 36.84 ± 0.71 | | |
| | 50 | 53.54 ± 0.47 | | |
| | 100 | 62.93 ± 0.44 | | |
| Pioglitazone | 6.25 | 23.46 ± 0.67 | 61.28 | -7.1 |
| | 12.5 | 29.76 ± 1.32 | | |
| | 25 | 35.98 ± 0.95 | | |
| | 50 | 48.65 ± 1.12 | | |
| | 100 | 63.58 ± 0.86 | | |
| Suramin | 6.25 | 36.68 ± 0.95 | 33.37 | – |
| | 12.5 | 40.60 ± 0.33 | | |
| | 25 | 50.60 ± 0.71 | | |
| | 50 | 62.56 ± 0.45 | | |
| | 100 | 68.60 ± 0.47 | | |

The *p*-nitro derivative (**TN05**) exhibited the highest interactions at the receptor active site through a conventional hydrogen bonding between indole N-H and Gln262, pi-pi stacking with Phe182, pi-alkyl interaction with Val49, pi-sigma interaction with Ala 217 and van der Waals interactions with residues Arg24, Ala27, Tyr46, Asp48, Asp181, Ser216, Ile219, Gly220 and Gly259 (Fig. 3b). The *p*-chloro derivative (**TN07**) showed interactions with the receptor active site through a conventional hydrogen bonding Arg24, pi-alkyl interaction with Val49, Phe182, Ala217 and Met258, pi-sigma interaction with Tyr46 and Met258, van der Waals interactions with residues Asp48, Ile219 and Gly220.

## Conclusion

The study report highlights the successful synthesis of a new series of indole-substituted thiazolidinediones (**TN01-TN08**) with good yields. The chemical structures of all analogues were elucidated using FTIR, $^{1}H$ NMR, $^{13}C$ NMR,

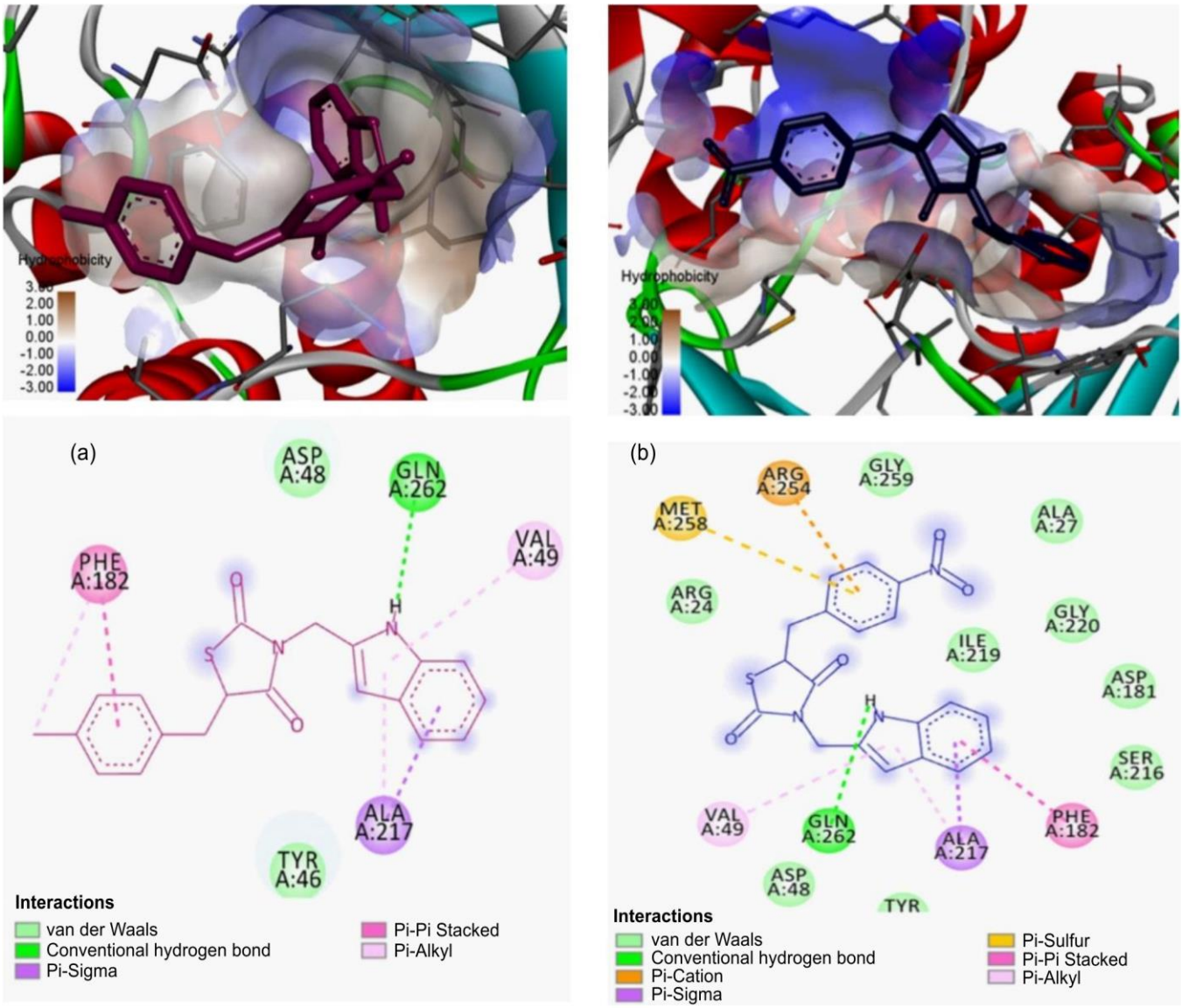


Fig. 3. (a and b) Binding pose and two-dimensional interactions of compounds **TN04** and **TN05** within the active loop of PTP1B enzyme

mass spectrometry and melting point analysis. Further, molecular docking simulation provided valuable insights into ligand potency and binding affinities of these ligands at the active site of PTP1B enzyme. As a preliminary screening method, the MTT assay was conducted for the synthesized compounds to compare the cell viability. A colorimetric GOD-POD assay was conducted on L6 cells treated with test compounds to evaluate the efficacy in enhancing glucose uptake. Based on these preliminary screening results, the selected analogues were evaluated for their ability to inhibit Protein Tyrosine Phosphatase 1B enzyme. Most of the synthesized compounds tested showed moderate to good PTP1B inhibition. Notably, compounds **TN04** and **TN05** exhibited significant cell viability, glucose uptake and PTP1B enzyme inhibition with an assured enhancement in insulin sensitivity. Further studies using animal models are necessary to confirm the potency and comprehensive anti-diabetic activity of these compounds, as well as their toxicity profiles.

## ACKNOWLEDGEMENTS

The authors are grateful to Management, Dr. Moopen's College of Pharmacy, Wayanad, India for providing the research facilities.

## CONFLICT OF INTEREST

The authors declare that there is no conflict of interests regarding the publication of this article.

## REFERENCES

1. Standards of Care in Diabetes–2023 Abridged for Primary Care Providers, *Clin. Diabetes*, **41**, 4 (2023); https://doi.org/10.2337/cd23-as01
2. S. Chatterjee, K. Khunti and M. J. Davies, *The Lancet*, **389**, 2239 (2017); https://doi.org/10.1016/S0140-6736(17)30058-2
3. D. L. Morris and L. Rui, *Am. J. Physiol. Endocrinol. Metab.*, **297**, E1247 (2009); https://doi.org/10.1152/ajpendo.00274.2009

4. B. A. Babalola, M. Malik, O. Olowokere, A. Adebesin and L. Sharma, *Eur. J. Med. Chem. Rep.*, **13**, 100252 (2025); https://doi.org/10.1016/j.ejmcr.2025.100252
5. G. Bansal, P.V. Thanikachalam, R.K. Maurya, P. Chawla and S. Ramamurthy, *J. Adv. Res.*, **23**, 163 (2020); https://doi.org/10.1016/j.jare.2020.01.008
6. M.G. Srinivasa, J.G. Paithankar, S.R. Saheb Birangal, A. Pai, V. Pai, S.N. Deshpande and B.C. Revanasiddappa, *RSC Adv.*, **13**, 1567 (2023); https://doi.org/10.1039/D2RA07247E
7. V. Sridhar and H. Park, *New J. Chem.*, **44**, 5666 (2020); https://doi.org/10.1039/C9NJ05822B
8. L. Chen and Y.H. Kang, *J. Funct. Foods*, **5**, 981 (2013); https://doi.org/10.1016/j.jff.2013.01.008
9. S. Edirs, L. Jiang, X.L. Xin and H.A. Aisa, *J. Pharmacol. Sci.*, **137**, 212 (2018); https://doi.org/10.1016/j.jphs.2018.06.011
10. K. Kavitha, K. Sujatha and S. Manoharan, *J. Nanomed. Biother. Discov.*, **7**, 152 (2017); https://doi.org/10.4172/2155-983X.1000152
11. K. Varshney, A. K. Gupta, A. Rawat, R. Srivastava, A. Mishra, M. Saxena, A. K. Srivastava, S. Jain and A. K. Saxena, *Chem. Biol. Drug Des.*, **94**, 1378 (2019); https://doi.org/10.1111/cbdd.13515
12. Y. Saidu, S. Muhammad, A. Yahaya, A. Onu, I. Mohammed and L. Muhammad, *J. Intercult. Ethnopharmacol.*, **6**, 154 (2017); https://doi.org/10.5455/jice.20161219011346
13. P. Joshi, G.S. Deora, V. Rathore, O. Tanwar, A.K. Rawat, A.K. Srivastava and D. Jain, *Med. Chem. Res.*, **22**, 28 (2013); https://doi.org/10.1007/s00044-012-0007-0
14. T. Kostrzewa, J. Jończyk, J. Drzeżdżon, D. Jacewicz, M. Górska-Ponikowska, M. Kołaczkowski and A. Kuban-Jankowska, *Int. J. Mol. Sci.*, **23**, 7034 (2022); https://doi.org/10.3390/ijms23137034
15. P. Rath, A. Ranjan, A. Ghosh, A. Chauhan, M. Gurnani, H.S. Tuli, H. Habeeballah, M.F. Alkhanani, S. Haque, K. Dhama, N.K. Verma and T. Jindal, *Molecules*, **27**, 2212 (2022); https://doi.org/10.3390/molecules27072212
16. G.M. Morris, R. Huey, W. Lindstrom, M.F. Sanner, R.K. Belew, D.S. Goodsell and A.J. Olson, *J. Comput. Chem.*, **30**, 2785 (2009); https://doi.org/10.1002/jcc.21256
17. S. Forli, R. Huey, M.E. Pique, M.F. Sanner, D.S. Goodsell and A.J. Olson, *Nat. Protoc.*, **11**, 905 (2016); https://doi.org/10.1038/nprot.2016.051
18. A. Shivamurthy Harisha, K. Nagarajan, S. Saravanan, V. Manohar, S.P. Thomas and T. Narasingarow Guru Row, *Results Chem.*, **4**, 100376 (2022); https://doi.org/10.1016/j.rechem.2022.100376
19. S.K. Gupta, Z. Singh, A.J. Purty and M. Vishwanathan, *Int. J. Diabetes Dev. Ctries.*, **29**, 166 (2009); https://doi.org/10.4103/0973-3930.57348
20. S. Amin, K.A. Sheikh, A. Iqubal, M.A. Khan, M. Shaquiquzzaman, S. Tasneem, S. Khanna, A.K. Najmi, M. Akhter, A. Haque, T. Anwer and M. Mumtaz Alam, *Bioorg. Chem.*, **134**, 106449 (2023); https://doi.org/10.1016/j.bioorg.2023.106449